
⁵⁴Xe and ³⁶Kr gas filled proportional counters and characteristic X-rays detection

Hemn, Muhammad Salh, Ari, Maghdid Hamad*

Department of Physics, Koya University, Koya, Kurdistan Region, Iraq

Email address:

hemn.salh@koyauniversity.org (Hemn M. S.), ari.hamad@koyauniversity.org (Ari M. H.)

To cite this article:

Hemn, Muhammad Salh, Ari, Maghdid Hamad. ⁵⁴Xe and ³⁶Kr Gas Filled Proportional Counters and Characteristic X-Rays Detection. *American Journal of Physics and Applications*. Vol. 2, No. 4, 2014, pp. 95-103. doi: 10.11648/j.ajpa.20140204.12

Abstract: This study examines several important features of characteristic X-rays, including their production, spectroscopy and interactions with materials. Characteristic X-rays for different elements (²⁹Cu, ⁴²Mo, ⁴⁷Ag, ⁵⁶Ba and ⁶⁵Tb) were obtained from a variable energy X-ray source by using gamma rays around 60 keV from ²⁴¹Am. It was found that the energy and intensity of generated characteristic X-ray photons are proportional to the atomic number of the targets within the variable energy X-ray source. In addition, X-ray spectroscopy for such targets was investigated by using two gas- filled (⁵⁴Xe and ³⁶Kr) proportional counters. Furthermore, it was discovered that the probability of photoelectric absorption of (⁵⁴Xe) gas-filled proportional counter is almost 1.5 times higher than the probability of photoelectric absorption of (³⁶Kr) gas-filled proportional counter.

Keywords: Proportional Counters, Characteristic X-Ray, Detection Efficiency

1. Introduction

X-rays are high-frequency, short-wavelength electromagnetic radiation containing invisible photons, and they are located between ultraviolet and gamma rays on the electromagnetic spectrum. Producing X-rays can be clearly understood by using Bohr atomic model, which describes the composition of an atom. According to this model, the nucleus of an atom consists of positively charged protons and neutrons which have a neutral electric charge. The nucleus is surrounded by electrons and the number of negatively charged electrons is equal to the number of the protons in a non-ionized and neutral atom. Moreover the maximum number of electrons in each shell is given by:

$$\text{The maximum number of electrons in a shell} = 2.n^2$$

Where n is the number of the shell and n= 1, 2, 3... for the first, second and third shell,...respectively (Fosbinder and Orth, 2011).

Electrons make a circular movement within the shells around the nucleus of the atom at different angles along complex pathways. Electrons are holed by the nucleus because they have binding energy (E_b) provided by the atom itself. In addition, the binding energy decreases as the distance between nucleus and electrons increases. In

contrast, the potential energy difference (ΔE) between shells goes up as their distance from the nucleus increases.

X-rays are primarily created via two mechanisms, namely Bremsstrahlung radiation and characteristic X-rays. Bremsstrahlung radiation is a German term meaning "breaking radiation", and in this process a fast-moving charged particle (electron) interacts with the nucleus of an atom rather than interacting with the orbital electrons. It is clear that in this kind of interaction the electrical field of the nucleus is attempting to deflect the moved charged particle. This deflection results in a deceleration of the accelerated charged particle, and the amount of kinetic energy lost by the electrons produces a Bremsstrahlung photon. The energy of this photon depends on the degree of energy possessed by the charged particle which strikes the nucleus. The second mechanism, which is the main process for producing the used characteristic X-rays in this study, will be explained further in the theory part of this paper (Van Grieken and Markowicz, 2001).

Presently, X-rays are widely used in many sections of life, including security screening systems, tomography, diagnostic uses, non-destructive tests and so on. Radiographic non- destructive tests which use X-rays are one of the tests which are used to inspect the internal parts of objects. For example, they can be used in nuclear energy power plants to inspect pipeline welds or pressure vessels

because the intensity of their photons can be changed, and they can also be switched off when such action is required (Prekeges, 2012 and Hertrich, 2005).

2. Theory

2.1. Characteristic X-Rays

In 1895, X-rays were discovered by Roentgen while he was conducting an experiment in a darkened room. He noticed that some equipment, which had been used in an experiment, fluoresced by an unknown ray; as such, he used the term “X-ray”. Furthermore, he noticed that the ray was produced when a beam of electrons struck the material. In time he discovered that the X-ray penetrating power and their absorption in targets such as aluminum. Characteristic X-rays are those X-rays produced when electrons are transited between atomic shells and rearrange themselves following excitation. Excitation may be the result of radioactive decay or an external radiation. Characteristic X-rays energy is equal to the energy difference between the two shells between which the electrons transited. Each element has a different binding energy with other atoms, and therefore is called characteristic x-ray (Krane, 1988). In this study an external radiation source (^{241}Am) is used to generate characteristic X-rays for different targets (Ag, Cu, Mo, Tb and Ba). Americium-241 decays into four excited states and a ground state of neptunium-237 with an approximate half- time of 432 years. This decay occurs through the emission of five various alpha particles from americium-241. Finally, gamma rays with virtual energy (60 keV) are produced when the excited states of the neptunium-237 approach the ground state through the various excited states outlined below.

According to the classic Bohr model of the atom, electrons are located in the orbitals of an atom with particular quantized energy levels. The nucleus of the atom

binds electrons through charge-charge interactions. Electrons in the inner shell (K) have maximum binding energy compared with other outer shells (L, M...); in order to obtain characteristic X-rays, the energy of the incident radiation must be higher than the binding energy of orbital electrons will not occur. The process of producing X-rays such as variable energy X-rays source can be explained in a number of steps. Firstly, when an electron in a K-shell is excited by bombarding radiation, it is transited, following which a temporary vacancy appears in the atom’s K-shell. Immediately, this vacancy is filled by electrons coming from the other outer shells, and a characteristic K X-ray is produced. If the electron moves from the L-shell, it will result in a K_{α} photon, and its energy would equal the difference between the binding energy of the K and L shells. In addition, K_{β} X- rays can be generated via the same mechanism, but this time the electron comes from the M-shell and its energy equals the difference between the binding energies of the K and M shells, as shown in the diagram below (1-2) (Knoll, 2000).

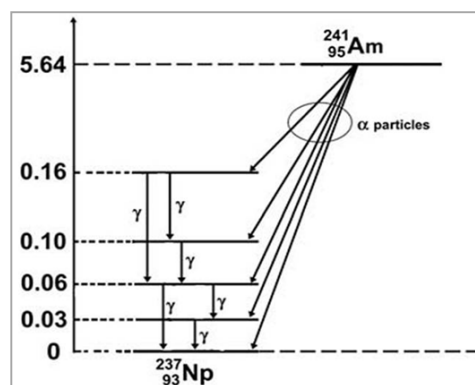


Figure (1-1). Schematic decay of ^{241}Am into ^{237}Np , taken from (http://www.nap.edu/openbook.php?record_id=11976&page=2).

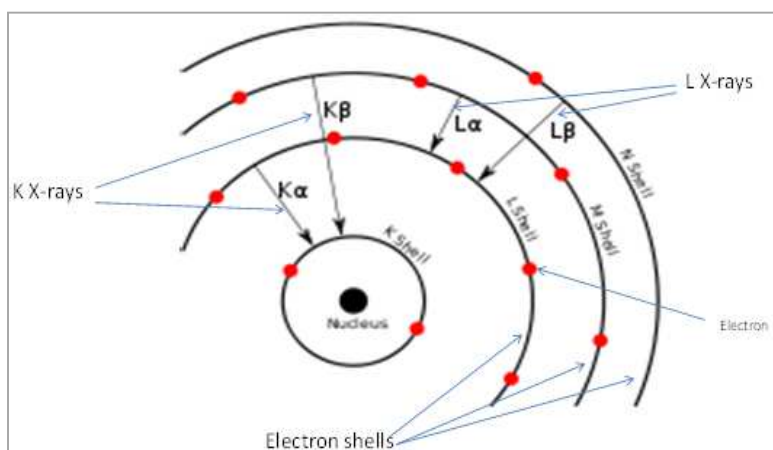


Figure (1-2). Illustration of the process of generating K and L X-rays inside an atom. Taken from http://www.thefullwiki.org/X-ray_generation

2.2. Proportional Counters

A proportional counter is a sort of gas-filled detector discovered in the late 1940s. Such counters are used in

certain radiation detection situations, particularly when the initial number of created electron-ion pairs from the incident ionizing radiation is too small. For this reason they have been used in this experiment to study and investigate

the spectroscopy of X-rays that have low energies. It can be said that the most common geometry for proportional counters is a cylindrical geometry because the electric field increases in the same direction that the electrons move towards the anode, as shown in figure (1-3) (Webster and Eren, 2014). Where the central wire (anode electrode) is enclosed by a cylindrical cathode, the space between the central wire and cylindrical cathode is usually filled with a mixture of 90% noble gas (which would be fairly nonreactive and have a complete valence shell) and a very small amount (10%) of a polyatomic quench gas, such as methane, for quenching purposes. In some configurations a very thin window is built either into the wall of the counter or at the end of the counter with a material that has a low atomic number, such as beryllium ($Z=4$), in order to minimize absorption of the incident radiation in the wall (L'Annunziata, 2012).

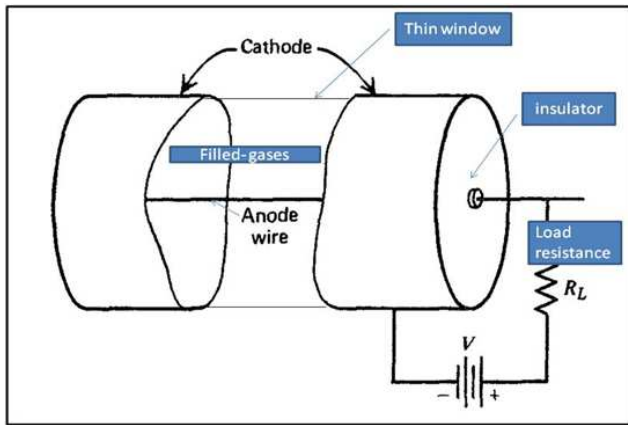


Figure (1-3). Basic composition of a gas-filled proportional counter, taken from (Knoll, 2000).

Following the creation of electron-ion pairs from the incident radiation, electrons move towards the anode-collecting electrode, and the holes move towards the cylindrical cathode electrode under the influence of the supplied electric field. Proportional counters depend on a gas multiplication mechanism for their operation, which is the result of raising the applied electric field to the counters. At a sufficient value of the electric field, the released electrons may gain significant kinetic energy from the electric field, and when they collide with the gas molecule they produce more electron-ion pairs. As this chain of creation continues more and more ionization is obtained, a process which is known as "Townsend avalanche". Secondary ionization will occur if the applied electric field is greater than the threshold value, which is typically around 10 V/m for most gases under atmosphere pressure. The total charge produced in the counter is given by:

$$Q = \frac{E e M}{W} \quad (1.1)$$

Where E is the deposited energy within the detector from radiation, W is the required energy for creating an electron-ion pairs (about 30 eV), e is the electron charge and M is

the multiplication factor and its typical value (10^3 - 10^4). Furthermore, the total number of collected charges is proportional to the initial number of ion pairs and the energy of the incident radiation. Xe, Kr, Ar gases are used to fill the detector because the ability of these counters in the spectrometry of photons depends on the atomic number of the gas inside the detector. (Knoll, 2000 and Krane, 1988):

2.3. Interactions of Characteristic X-Rays with (Xe and Kr) Filled-Gas Counters

In general, photon radiation (X-rays and gamma rays) interact with substances via three mechanisms, namely pair production, Compton scattering and the photoelectric effect. In each mechanism the incident photon will either deposit all of its energy or else lose a particular amount of its energy. Furthermore, each mechanism can be considered as the predominant interaction in specific circumstances. For example, pair production can be observed when the energy of the incident photon is significantly greater than the combined remaining mass of (e^- and e^+), which is around (1022 keV). In this work, photoelectric absorption can be seen as the predominant interaction mechanism because the generated characteristic X-rays have low energies. In the photoelectric absorption process the energy of characteristic X-rays may be entirely absorbed by an atom. The deposited energy is transferred to an orbital electron, and then the electron is ejected. The energy of released electron is given by:

$$E_e = E_{x\text{-ray}} - E_b \quad (1.2)$$

Where $E_{x\text{-ray}}$ is the energy of the incident X-rays and E_b is the binding energy of electron (Turner, 2008).

The binding energy of electrons in outer shells is lower than the inner shells because it is dependent on the atomic number Z of the atom as well as the electron shell. The approximate binding energy for the K, L and M shells can be calculated by these formulae:

$$E_b (\text{K-shell}) \approx Ry (Z - 1)^2 \quad [\text{eV}] \quad (1.3)$$

$$E_b (\text{L-shell}) \approx \frac{1}{4} Ry (Z - 5)^2 \quad [\text{eV}] \quad (1.4)$$

$$E_b (\text{M-shell}) \approx \frac{1}{9} Ry (Z - 13)^2 \quad [\text{eV}] \quad (1.5)$$

Where Ry is Rydberg's energy = 13.61 eV (Leory and Rancoita, 2004)

Photoelectron absorption also creates characteristic X-rays because of coming electrons from outer shells filling the vacancy in inner shells. The aim of using Xe and Kr gas-filled proportional counters in this experiment is to study how their photoelectron absorption cross-sections are different because:

$$\text{Their photoelectron absorption cross section } \propto \frac{Z^4}{E^{3.5}} \quad (1.6)$$

Moreover, in photoelectric absorption Auger electron

may appear because when an electron transits between two shells to fill a vacancy, an amount of energy will be released. This energy can be absorbed by a bound electron of a higher shell, causing an electron ejection. This ejection

is called an Auger electron, and was discovered in 1925 by Pierre-Victor Auger, hence the name. The whole process is shown below in figure (1-4) (Gilmore, 2008).

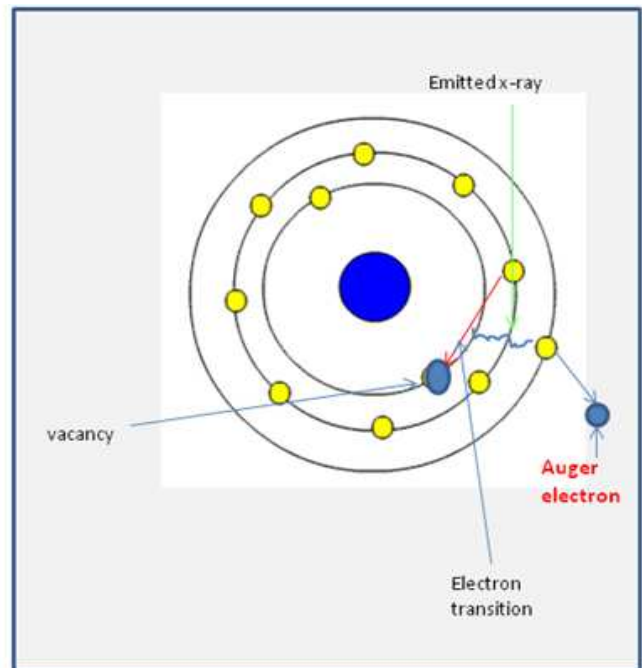
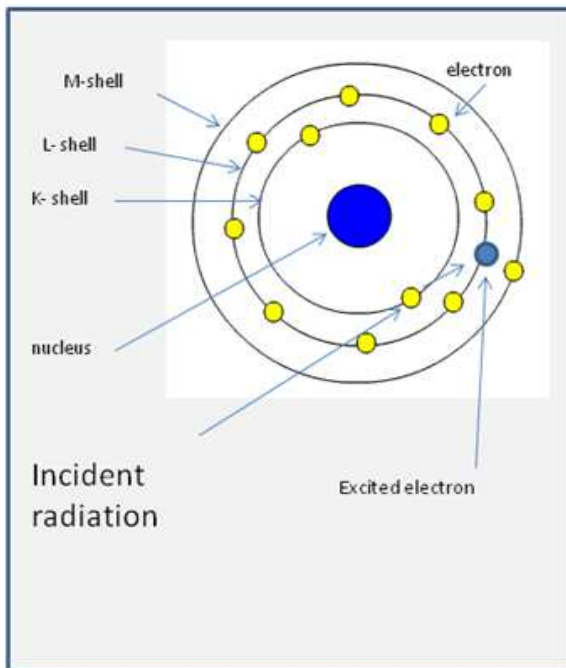


Figure (1-4). the process of Auger electron emission (http://www.safetyoffice.uwaterloo.ca/hse/radiation/rad_sealed/matter/atom_structure.htm)

2.4. Electronics

The first equipment in an output pulse processing chain of a nuclear radiation detector is a preamplifier. As can be deduced from its name, the word “preamplifier” means “before amplifier”, and therefore it does not work as an amplifier. Rather, it collects the charges generated within a counter. Besides this, it is used as interference between the signal process apparatus that comes after the amplifier, and the radiation detection detector. The preamplifier has three basic functions: to modify the output signal of the counter to a voltage signal, and to amplify and shape the pulse. Preamplifiers can be divided into three main categories, namely current sensitive, voltage sensitive and charge sensitive preamplifiers. They require two essential bases which are, firstly, that they must be placed as close as possible to the detector in order to maximize the signal to noise ratio. Secondly, it is important that they have a significant high- impedance load for the radiation detector since this helps where there is a low impedance supplier for the amplifier. After this process is completed by a preamplifier, the signal transfer to the main amplifier via

cables will then be reshaped and amplified the pulse as required (Leo, 1994 and Tsoufanidis, 1993).

3. Methodology

3.1. Characteristic X-Rays Production and Energy Resolution

The instruments of the experiment were connected together. The proportional counter connected to a preamplifier, to a spectroscopy amplifier and to an EASY-MCA (multi-channel analyzer) as shown in the figure (2-a). In this part of the experiment the characteristic X-rays-generated for five various targets, which have different atomic numbers (^{29}Cu , ^{42}Mo , ^{47}Ag , ^{56}Ba and ^{65}Tb) from a variable energy X-ray source (identification: ANS30). The source consists of ^{241}Am , that is a virtual (60 keV) gamma-ray emitter with approximate activity (350 MBq) (Gilmore, 2008). The five targets rotated on a rotary holder around the radioactive source when someone attempts to obtain variable characteristic X-rays as shown in the figure (2-a).

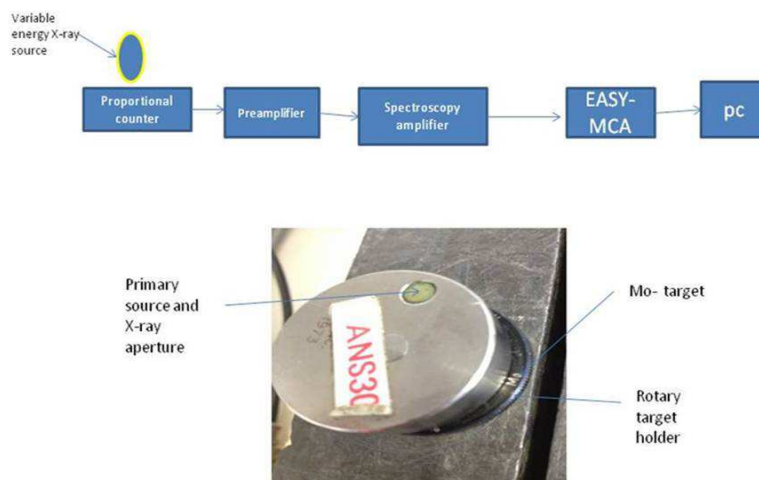


Figure (2-a). a block diagram of the experiment and the variable energy X-ray source.

In order to observe the operational voltage for the both gas-filled proportional counters (^{36}Kr and ^{54}Xe gases), the variable energy X-ray source for Cu target was placed on the side of the shield which surrounds the counters. Following this, the energy resolution of the detectors was calculated by reading and recording the full width at half maximum (FWHM) for the peak from the incident of Cu characteristic X rays into the counters through a thin window at the side of the detectors. Furthermore, information about how this calculation was obtained will be described in the results and discussion sections of this paper.

3.2. Energy Calibration

The operational voltage for both Kr and Xe proportional counters was found in the first part of the experiment. This voltage remained constant and was applied to the other parts of this experiment such as calibration and efficiency comparison of the counters. The gain of the amplifier and shaping time were 50 and $2\mu\text{s}$ respectively and they kept at the same value as the energy resolution part. This time, targets within the variable energy X-ray source were rotated, and for each target the detection of produced characteristic X-rays was carried out for a period (500 s) of live time. Then, the channel number at which the K_α peak was obtained was recorded, as shown in figure (2-b). However, the energy of the K_α x-ray peak was determined from the Table of Isotopes This procedure was repeated twice for each target and for all the five elements (Cu, Mo, Ag, Ba and Tb). The reasons for selecting the parameters, and the calculated results, are explained in the results and discussion parts of this report.

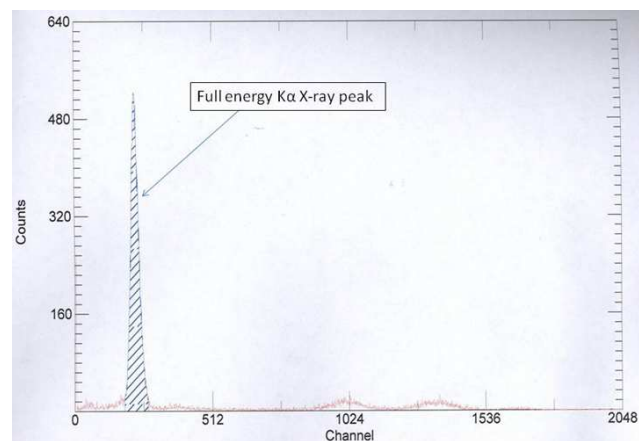


Figure (2-b). Spectrum obtained from the X-ray variable source using Cu target.

3.3. Kr and Xe Proportional Counter Efficiencies

The final part of the work examined another vital future of the counters, namely the ability of the counters to detect radiation. To investigate this point, part 2 of the experiment was repeated but this time the gross area from the output spectrum for the K_α x-rays was recorded using the same conditions of the instruments. Then, the count rates for the same target by the two detectors were obtained. There was an attempt to find either the absolute or intrinsic efficiency of the counters, but this was impossible because the activity of the targets was unknown. Each target was used first with a Kr and then an Xe detector, both of which had the same shape and geometry. The results are shown in the next part of the report.

4. Results

4.1. Energy Resolution

As mentioned in the experimental procedure section of this report, characteristic X-rays from Cu target were used

for studying the energy resolution of the counters. At each value of the applied voltage for both Kr and Xe counters, the full width at half maximum (FWHM) and the peak centered channel number(H_0) for the full energy K_{α} X-ray peak was recorded from the produced spectrum from Cu target, as shown in table(1.1). After that, the energy resolution was calculated by using the equation below:

$$\text{Energy resolution (R) \%} = \frac{FWHM}{H_0} \times 100$$

(Johansen and Jackson, 2004)

Table(1.1). Energy resolutions for Kr and Xe proportional counters from Cu target

Voltage(volts)	(H_0)-Kr	FWHM	R%	(H_0)-Xe	FWHM	R%
900	129.45	13.36	10.32	42.46	8.51	20.04
920	163.83	16.14	9.852	54.79	9.85	17.98
940	194.74	18.4	9.448	68.52	11.6	16.93
960	242.27	22.8	9.411	84.31	13.48	15.99
980	313.05	29.4	9.391	103.75	15.61	15.05
1000	381.33	35.75	9.375	130.43	19.15	14.68
1020	457.9	42.5	9.282	152.5	20.68	13.56
1040	586.63	54.87	9.353	190.67	27	14.16

Finally, graphs were plotted between the voltage and energy resolution for both counters and the operational voltage was considered to be 1020 volts for both. The discussion section provides more about the reason behind selecting this particular voltage.

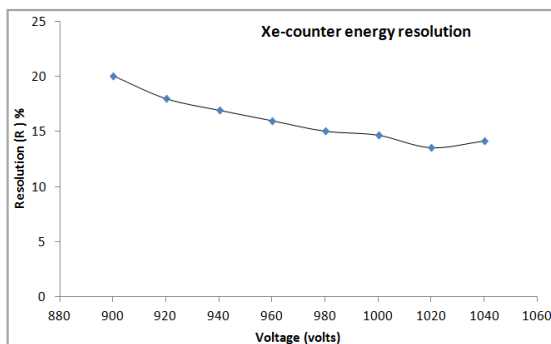
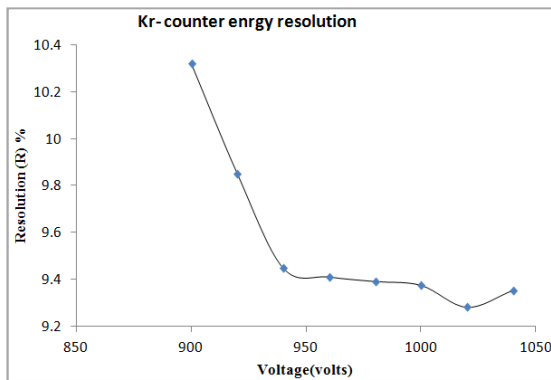


Figure (3-a). Energy resolution of the counters against applied voltage

4.2. Energy Calibration

The system was calibrated by utilizing five elements (^{29}Cu , ^{42}Mo , ^{47}Ag , ^{56}Ba and ^{65}Tb) of the variable energy X-

ray source. These targets have different atomic numbers, and as such they generate various energy characteristic X-rays as shown in figure (3-b).

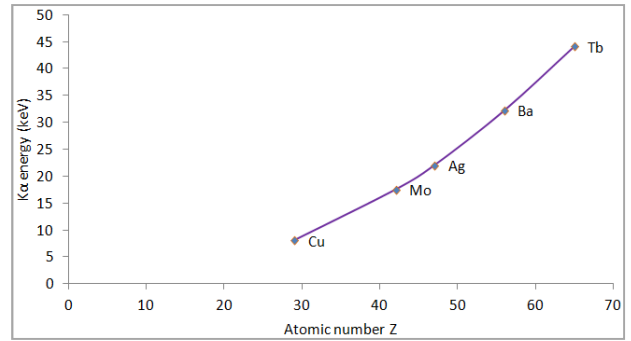


Figure (3-b). Average K_{α} energy for the different elements against their atomic number.

Their K_{α} X-ray energy was calculated by taking the average energy of $K_{\alpha 1}$ and $K_{\alpha 2}$ X-rays from the Table of Isotopes, because the difference between $K_{\alpha 1}$ and $K_{\alpha 2}$ was very small. Since the operational voltage was found for Kr and Xe proportional counters, for this part of experiment the voltage was set at 1020 volts for both counters. Following that, the channel number for each full energy peak of K_{α} X-ray was recorded; all details are shown in table(1.2). Also, a graph was plotted to show how the energy of each target was proportional to its atomic number as well as its energy, and it was found that

$$\text{Full peak energy (keV)} = (0.023 \times \text{channel number}) - 0.0584 \quad \text{for Kr- detector}$$

$$\text{Full peak energy (keV)} = (0.0393 \times \text{channel number}) - 0.0584 \quad \text{for Xe- detector}$$

Table(1.2). The average energy of ($K_{\alpha 1}$ and $K_{\alpha 2}$) of the variable energy X-ray source targets and channel numbers

Targets	Atomic number	K_{α} X-ray energy(keV)	Channel number Kr- counter	Channel number -Xe counter
Cu	29	8.038	355.02±0.23	206±2
Mo	42	17.48	763.32±0.18	455.5±2.5
Ag	47	22	965.86±0.28	576±4
Ba	56	32.19	1388.12±0.12	826±2
Tb	65	44.11	1931±0.27	1126.5±0.5

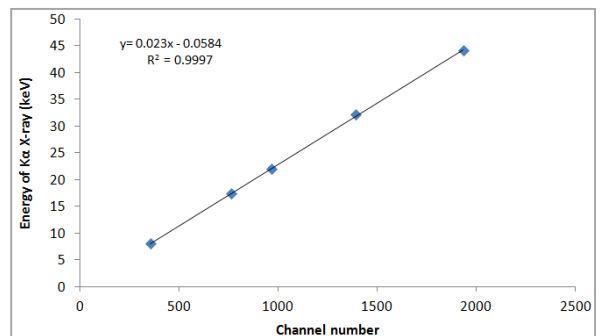


Figure (3-c). Energy of K_{α} X-rays against channel numbers for Kr-detector

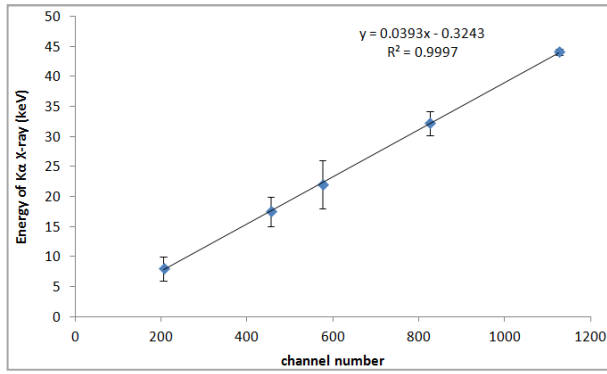


Figure (3-d). Energy of Kα X-rays against channel numbers for Xe-detector

The final part of the study was carried out to investigate how the efficiency of the counters differ. It was found that the ability of the Xe-proportional counter is greater than the Kr-counter's ability by a factor which is greater than 1.5 (see discussion). The voltage was set at 1020 volts for both detectors, and each measurement ran for a period of 500s of live time. During this work, the net area counts were found by subtracting the background counts from the measured gross area counts of each spectrum for Kα X-ray full energy peak of each targets. Then obtained net area counts were divided by the live time to obtain count rates for each detectors. At the end, count rates measured by Xe-proportional were divided by the count rates detected by Kr-gas filled proportional detector. Several graphs plotted the achieved results as shown below.

4.3. Kr and Xe Proportional Counter Efficiencies

Table (1.3). Detected count rates by Xe and Kr counters and the ratio between them.

Targets	Atomic number	Kα X-ray energy(keV)	Kr- counter count rate (cps)	Xe- counter count rate (cps)	Ratio of Xe- detector count rates to Kr- detector count rates
Cu	29	8.038	113.72±0.49	173.56±0.6	1.52±0.0084
Mo	42	17.48	396.04±0.89	635.4±1.13	1.6±0.005
Ag	47	22	382.97±0.88	598.32±1.1	1.56±0.0045
Ba	56	32.19	193.55±0.63	316.36±0.8	1.63±0.0067
Tb	65	44.11	205.7±0.65	327.36±0.81	1.59±0.0064

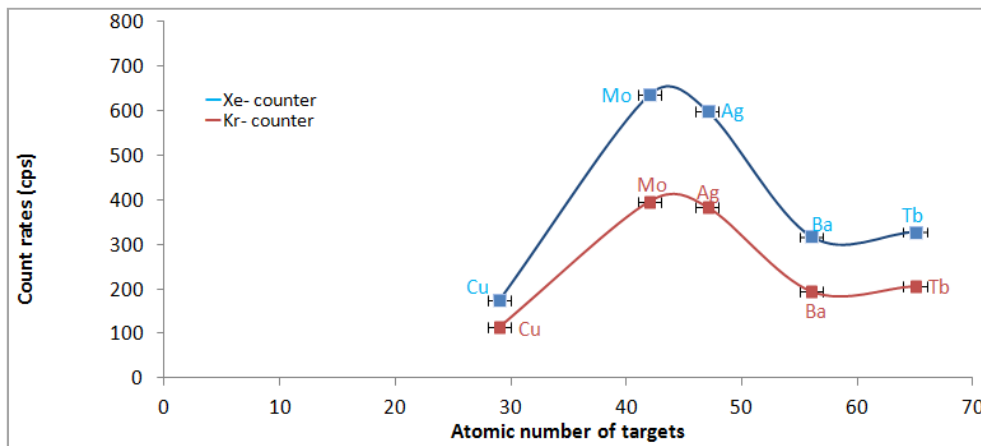


Figure (3-e). Count rates for both counters against the atomic number of targets of variable energy x-ray source

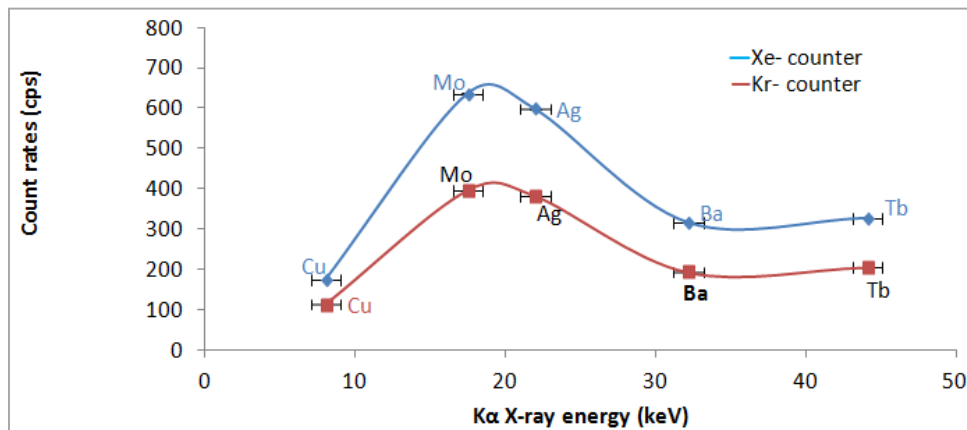


Figure (3-f). Count rates for both counters against Kα X-rays energy from the targets

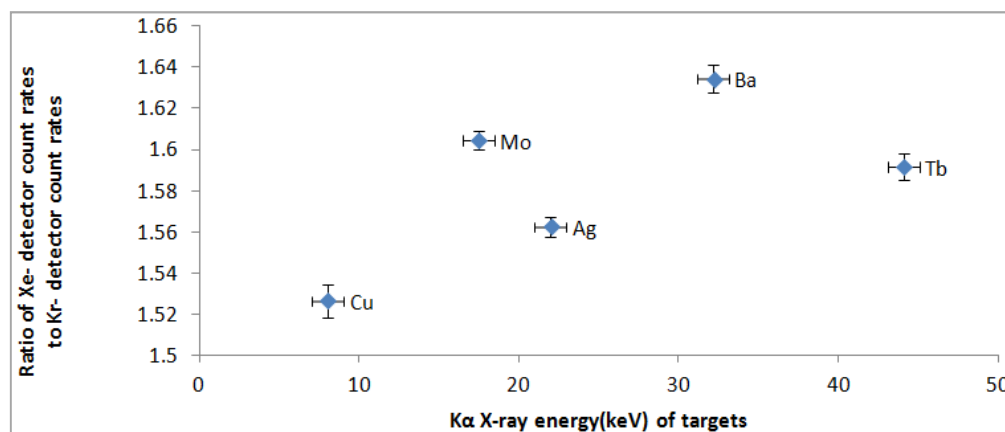


Figure (3-g). The ratio of count rates against the K α X-rays energy from characteristic x-ray source targets

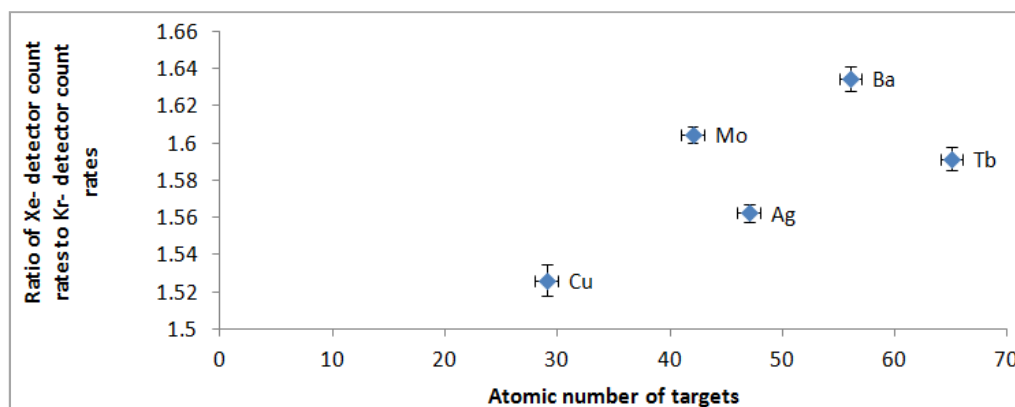


Figure (3-h). the ratio of count rates against the atomic number of characteristic x-ray source targets

5. Discussion and Conclusion

The operational voltage for both proportional counters was selected as (1020 V) because at this voltage the lowest value of energy resolution is obtained, as shown in figure (3-a). It is clear that energy resolution is the ability of a detector to distinguish two or more energy peaks which have almost the same energy and which appear close together. According to Knoll (2000) the small value of energy resolution, illustrates that the detector can recognize and differentiate between two peaks with close energy. However, higher magnitudes of energy resolution indicate that the detector produces the same response for a number of close peaks together. Turner (2008) has stated that the output signal of proportional counters is proportional to the number of electron-ion pairs produced within the counter and the incident radiation energy. When x-ray incidents a detector, the gas inside of a detector is ionized; as a result electrons and ions are produced. Moreover, in the proportional region electrons gain enough kinetic energy from the supplied electric field and they move towards the anode electrode, which in turn results in further ionisation through collision with the filled-gas molecules. The required time for collecting the formed electrons is smaller than 500ns. In contrast, it takes significantly longer for positive ions – around 10 μ s. Used proportional counters

have a thin window on one side. This window can be built at the end of the counters if the incident radiation energy is higher, because in this case the mean free path for stopping the incident radiation is increased in comparison to the side windows.

When the emitted gamma rays (60 keV) from the ^{241}Am , decaying process struck elements of the variable energy X-ray source, characteristic K α X-rays were obtained for each. It was observed that the elements have a higher atomic number as illustrated in figure (3-b). They generate higher characteristic X-rays, for instance ^{29}Cu has 8.083 keV while ^{65}Tb element has 44.11 keV characteristic X-rays. This difference is due to the difference in binding energy between elements; as noted before, the energy of the characteristic X-rays is equal to the difference between the binding energy between the two shells when the electron is ejected and the shell that sends an electron to fill the vacancy appears as a result of the electron ejection, as shown by Robinson (1974). The reason for this is that the increase in the positive charge of the nucleus with atomic number causes the electrons in all shells to be bound more tightly, and thus they have higher energy as Z increases. It seems that the lower energy characteristic X-rays may cause Auger electron emission.

The obtained spectrum for each target has a number of energy peaks, for example Mo element had three energy peaks: the first energy peak of Mo is understood to be the

characteristic $K\alpha$ X-rays for the element, the second peak is probably due to the characteristic X-rays from the filled gases (Xe and Kr) of the proportional counters and the third can be considered as being the result of the back scattered photon peak from ^{241}Am source. The more interesting spectrum was the Tb target spectrum because it had more than four peaks, the reason being that its atomic number is the highest, thus there is the probability of creating more than one characteristic x-ray peak from Tb.

It was also found that a Xe-gas filled proportional counter has a noticeably higher ability for detection produced characteristic x-rays from the variable energy X-ray source. This higher ability may occur for several reasons, one example being the energy of the incident radiation into the counters and the filled gases atomic numbers, because the photoelectric interaction is most likely to occur if the energy of the incident photon is just greater than the binding energy. Thus, it was noticed that counts detected by both counters have the highest value at a particular energy, but it then decreases and reaches a constant level when the energy of incident X-rays is further increased, as shown in the graph (3.f). Because both detectors are used for each characteristic X-ray, it therefore has a similar effect on their abilities. But the vital reason which played a significant role, which has supported by Millar (1974) is the atomic numbers of filled gases because by increasing their atomic number the probability of photoelectron absorption increases due to increased interaction with the molecules and less photon transmission through the higher atomic number gases, as shown in equation (1.2). It is clear that the atomic number of Xe is 54 and it is 1.5 times higher than the atomic number of Kr gas ($Z=36$) by using equ.(1.6) from Krane (1988). Hence the Xe gas-filled proportional counter count rates must have been bigger by 1.5 times rather than the count rates of Kr-gas counter. However, the observed results are between 1.52 and 1.63, as shown in table(1.3). This difference may be due to some limitations when conducting the experiment, for example using the ratio of count rates in spite of using the efficiency of counters to compare their abilities. However, trying to find either the absolute or intrinsic efficiency for the counters has been seen by some as complicated because the initial activity of the elements of the variable energy X-ray source are unknown. On the other hand, because we took the gross area counts for full peak energy from the spectrum, some of them seen to have combined the $K\alpha_1$ and $K\alpha_2$ characteristic X-rays and taken

the average for these two peaks from the Table of Isotopes.

References

- [1] Fosbinder, R., & Orth, D. (2011). Essentials of radiologic science. Lippincott Williams & Wilkins.
- [2] Gilmore, G. R. (2008) Practical gamma- ray spectrometry. 2nd edition. John Wiley & Sons, Ltd.
- [3] Hertrich, P. (2005) Practical radiography. John Wiley & Sons.
- [4] Johansen, G. A., & Jackson, P. (2004). Radioisotope gauges for industrial process measurements. John Wiley & Sons.
- [5] Knoll, G. F. (2000) Radiation detection and measurement. 3rd edition. John Wiley and Sons Inc.
- [6] Krane, K. S. (1988) Introductory nuclear physics. 3rd edition. John Wiley and Sons, Inc.
- [7] Leo, W. R. (1994) Techniques for Nuclear and particle physics experiments: A how-to approach. 2nd edition. Springer.
- [8] Leroy, C. and Rancoita, P. G. (2004) Principles of radiation interaction in matter and detection. World scientific publishing co. pte. Ltd
- [9] L'Annunziata, M. F. (Ed.). (2012). Handbook of radioactivity analysis. Academic Press.
- [10] Millar, R. H. (1975). Atomic number dependence of the photoelectric cross section for photons in the energy range from 4.5 to 25 keV. *J. Phys. B: Atom. Molec. Phys.*, Vol.8, No.12, 1975.
- [11] Prekeges, J. (2012) Nuclear medicine instrumentation. 2nd edition. Jones & Bartlett Publishers.
- [12] Robinson, J. W. (ed.) (1974) Handbook of spectroscopy. Vol I, CRC press.
- [13] Tsoufanidis, N. (1995) Measurement and detection of radiation. 2nd edition. Taylor and Francis.
- [14] Turner, J. E. (2008). Atoms, radiation, and radiation protection. John Wiley & Sons.
- [15] Van Grieken, R., & Markowicz, A. (Eds.). (2001). Handbook of X-ray Spectrometry. CRC Press
- [16] Webster, J. G., & Eren, H. (Eds.). (2014). Measurement, Instrumentation, and Sensors Handbook: Spatial, Mechanical, Thermal, and Radiation Measurement (Vol. 1). CRC press.